# Multifractal analysis for seismic wave in Kathmandu valley after Gorkha Earthquake-2015, Nepal

*B. R. Tiwari, J. Xu, B. Adhikari, N. P. Chapagain*

**Journal of Nepal Physical Society**

*Volume 6, Issue 2, December 2020*

*ISSN: 2392-473X (Print), 2738-9537 (Online)*

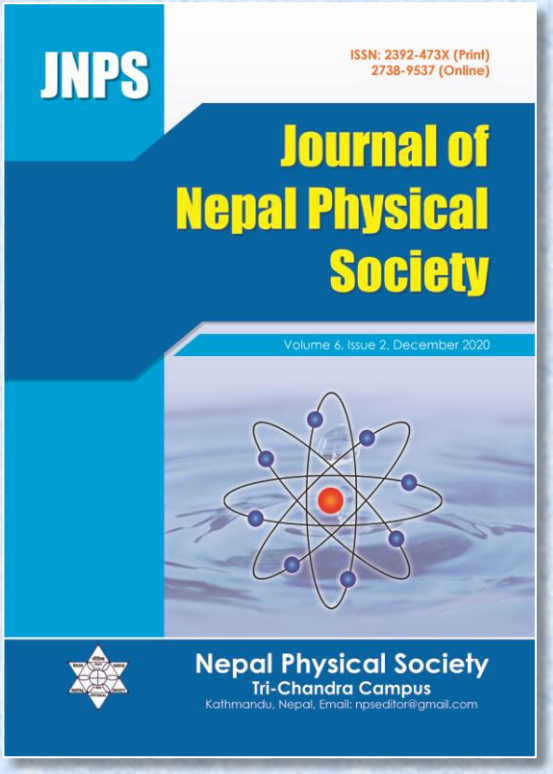




*JNPS*, **6** (2), 113-120 (2020)

DOI: http://doi.org/10.3126/jnphyssoc.v6i2.34866

**Published by:**

**Nepal Physical Society**

P.O. Box: 2934

Tri-Chandra Campus

Kathmandu, Nepal

Email: npseditor@gmail.com

*JNPS* ***6*** *(2): 113-120 (2020)*
*ISSN: 2392-473X (Print), 2738-9537 (Online)*

***Research Article*** *© Nepal Physical Society*
*DOI: http://doi.org/10.3126/jnphyssoc.v6i2.34866*

# Multifractal analysis for seismic wave in Kathmandu valley after Gorkha Earthquake-2015, Nepal

**B. R. Tiwari[1,*], J. Xu[1], B. Adhikari[2], N. P. Chapagain[3]**

[1]State Key Laboratory of Space Weather, National Space Science Center, Chinese Academy of Sciences, Beijing, China-100190

[2]Department of Physics, St. Xavier's College, Maitighar, Kathmandu, Nepal

[3]Department of Physics, Amrit Campus, Tribhuvan University, Kathmandu, Nepal

***Corresponding Email:** tiwari.baburam@gmail.com

***Received:*** *22 October, 2020;* ***Revised:*** *23 November, 2020;* ***Accepted:*** *26 December, 2020*

**Abstract**

We applied the multiscale signal processing technique, the Wavelet Transform Modulus Maxima (WTMM) to characterize high frequency properties of strong motion waveforms, in particular the temporal distribution and strength of singularities in Gorkha earthquake, 25th April 2015. We first explored their relation to earthquake data source. Then we applied the WTMM analysis to strong motion recordings. These showed that the timing and exponent of singularities measured by the WTMM method on the ground motion wave field are directly related to the position and exponent of assumed initial stress singularities on the fault plane. We found strong motion recordings at near the epicenter site have very high multifractality than far sites. Some differences and similarities among sites were successfully detected.

**Keywords:** Seismic waves, Strong ground motion, Singularity spectrum, Multifractal analysis.

## INTRODUCTION

Nepal is a mountainous country in the South Asia, which lies at the center of the 2500 km long Himalayan range. The entire Himalayan terrain and its surroundings is a highly active seismic zone on earth. Due to the active continental collision zone of the world the probability of earthquake occurrence is very high. The earthquake of 1934, 1980, 1988 and 2015 are the most destructive disasters which not only caused heavy losses to human lives and physical properties but also adversely affected the development process of the developing countries like Nepal [1]. During an earthquake, ground acceleration is measured in three different directions: vertically (V or Up-down) and two perpendicular horizontal directions north-south (NS) and east-west (EW). The peak acceleration in each of these directions is recorded. In earthquake research and engineering practice, the singularity spectrum is the standard tool for analyzing the signal [2, 3]. These multiscale techniques are well developed and have been applied in a variety of fields [4, 5]. In this paper, we have applied the multifractal spectrum approach to the analysis of four sets of strong ground motion at Kathmandu valley after the Gorkha earthquake 2015, Nepal. We applied this technique to analyze strong motion data and earthquake source processes. The study focuses on the interpretation and explanation of the various temporal fractal patterns found in earthquake time series. WTMM approach is a method for detecting the fractal dimension of a signal. It can partition the time and scale domain of a signal into fractal dimension regions. This method is also referred to as a "mathematical microscope" due to its ability to inspect the multi-scale dimensional characteristics of a signal and possibly inform about the sources of these characteristics [6].

At local time 11:56:25 am NST of 25 April 2015, an earthquake of MW 7.8 struck at Nepal (www.usgs.gov/news/magnitude-78-earthquake-nepal-aftershocks). The epicenter was located at 28.230° N and 84.731° E, at the depth of 15 km. This epicenter of the earthquake was ~77 km northwest of Kathmandu (28.14°N, 84.70°E) valley.

This earthquake struck central Nepal devastating the region at the rim of the High Himalayan range and affecting Kathmandu valley, more than eight thousand deaths, and approaching 10 billion dollars of property damages. Earthquake tremors were felt in a very large area of ~2000 km from the epicenter. This earthquake was caused by a sudden thrust, or release of built-up stress, along the major fault line where the Indian plate carrying India, is slowly diving underneath the Eurasian Plat carrying much of Europe and Asia [7, 8, 9, 10]. The maximum ground movement observed along the fault was recorded at 7 m vertical displacement. The spatial and temporal complexity of the earthquake source is strongly affected by spatial heterogeneities of fault strength and stress, and has a major impact on the amplitude and spatial variability of ground motions in the near-field sites [2, 3]. Self-similarity arguments suggest that this complexity extends over a broad range of length scales. We quantify signatures of spatio-temporal rupture complexity in the high-frequency band of strong ground motion recordings. We also compare the ground motion waves among these high-frequency attributes and earthquake physics, specifically the spatial distribution and singular character of initial fault stress concentrations at different stations.

In this present work, we report the maximum as well as minimum of the singularities of seismic wave in Kathmandu valley after Gorkha earthquake on 25 April 2015. Some new findings are drawn by studying these seismic ground motions recording at four different sites of Kathmandu. In addition, we have used the WTMM approach that provides an alternative way of measuring the global effects of natural disasters such as earthquakes and tsunami.

## DATA AND METHODOLOGY

The datasets used in the present study were obtained from European-Mediterranean Seismological Centre (EMSC) webpage: (http://www.emsc-csem.org/ Earthquake/seismologist). php, Central Department of Geology, Tribhuvan University, University Grants Commission office, Bhaktapur, Kirtipur Municipility Office and Pulchowk Campus, Institute of Engineering, Patan. We downloaded the dataset from the webpage: www.strongmotion center.org for the study of ground motion. The data used in this study were collected at the stations known as KTP, TVU, PTN and THM located at about 75~80 km to the east of the epicenter. The details of the locations of four stations are given in Table 1 and in Figure 1. A more detailed description of the complete data has been given by previous studies [10, 11].

**Table 1: Earthquake recording station code and their location information. Station Code, Latitude, Longitude, Height (m) and Epicentral Distance (Km)**

| Earthquake recording Station Code | Latitude | Longitude | Height(m) | Epicentral Distance (km) |
|---|---|---|---|---|
| KTP | N27.68216 | E85.27259 | 1370 | 75.9 |
| TVU | N27.68179 | E85.28825 | 1320 | 77.0 |
| PTN | N27.68150 | E85.31896 | 1310 | 79.3 |
| THM | N27.68130 | E85.37705 | 1320 | 83.7 |

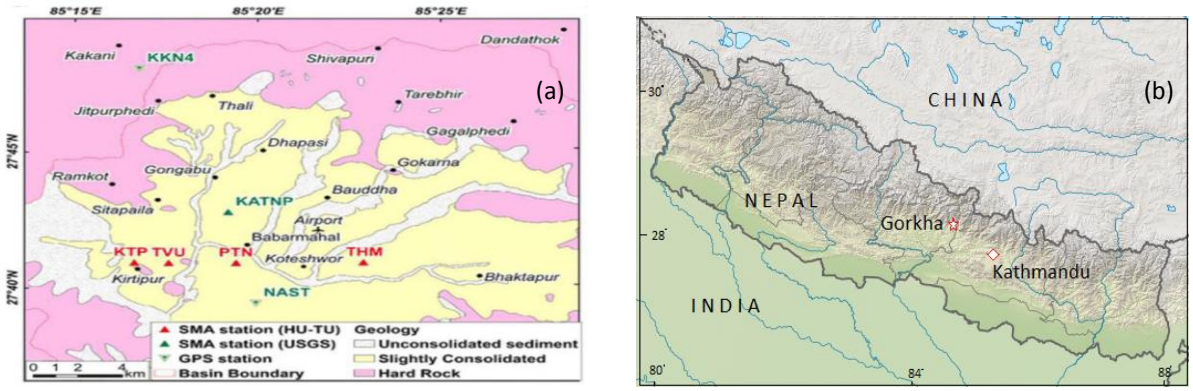


**Fig. 1:** (a) Location of the strong-motion seismometers measuring station and selected events in the Kathmandu [12]. (b) The red star shows the epicenter of the 2015 Gorkha earthquake (Modification from: https://en.wikipedia.org/wiki/April_2015_Nepal_earthquake)

## MULTIFRACTAL ANALYSIS

We have applied the wavelet-based approach to the analysis of four sets of earthquake data. In earthquake research and engineering practice, the singularity spectrum is the standard tool for analyzing the signal. We define strong phases in accelerograms as discrete occurrences of temporal singularities. A signal $f(t)$ with local singular behavior at $t_o$ can be locally expanded as the superposition of a smooth polynomial and a power law singularity:

$$f(t) \approx P_n(t-t_o) + O((t-t_o)^{\alpha(t_o)}) \quad \ldots\ldots\ldots (1)$$

where $\alpha$ is the local Hölder exponent characterizing the irregularities of the function $f$, and $P_n(t-t_o)$ is a polynomial of degree $n < \alpha(t_o)$. Higher positive value of $\alpha(t_o)$ indicates regularity in the function $f$. Negative $\alpha(t_o)$ indicates spike in the signal. If $n < \alpha < n+1$ it can be proved that the function $f$ is $n$ times differentiable but $n$ not $n+1$ times at the point $t_o$ [13]. All the Hölder exponents present in the time series are given by the singularity spectrum $f(\alpha)$. This can be determined from the Wavelet Transform Modulus Maxima (WTMM). We studied times-singularity spectrum distribution based on WTMM Method. By this method we analyzed the implementation of the time varying wavelet transform modulus maxima, including the wavelet type, selection of the scales, selection of the moment and the thresholding the maxima. These multiscale techniques are well developed and have been applied in a variety of fields. We applied this technique to analyze strong motion data and earthquake source processes.

The continuous wavelet transforms $W$ of a signal $f(t)$ is defined as

$$W_\psi(a,b) = \frac{1}{\sqrt{a}} \int f(t)\psi^*\left(\frac{t-b}{a}\right)dt \quad \ldots\ldots\ldots (2)$$

where $f(t)$ is the time series, $\psi(t)$ is the wavelet function and $*$ represents the complex conjugate. Here, $a$ and $b$ are real and $a > 0$.

Due to the variability pattern of our data, we have used the Morlet wavelet function given by

$$\psi(t) = e^{iKt}.e^{-t^2/2}$$

where K = 5 is recommended in practice but can be modified. The scaling and translation of this wavelet function are performed by the parameters $a$ and $b$. While the scale parameter $a$ stretches (or compresses) the mother wavelet to the required resolution, the translation parameter $b$ shifts the basic functions to the desired location.

The wavelet transform can reveal the local characteristics of $f(t)$ at a point $t_o$. More precisely, we have the following power-law relation:

$$W_\psi[f(t)](a,t_o) \approx |a|^{\alpha(t_o)} \quad \ldots\ldots\ldots\ldots\ldots (3)$$

where $\alpha(t_o)$ is the Hölder exponent (or singularity strength). We obtain the exponent $\alpha(t_o)$, for fixed location $t_o$, through the log-log plot of the wavelet transform amplitude versus the scale $a$.

The wavelet transforms of $f(t)$ can show the invariance with respect to some renormalization operations involving multiplicative cascades. This means that there is a hierarchy of the WTMM that has been used to define the partition function based on the multifractal formalism [14]. The local maxima of $|W_\psi(a,b)|$ at a given scale $a$, are likely to contain all the hierarchical distribution of singularities in the signal [13]. We have to identify a space-scale partitioning over the maxima distribution, and, consequently, a usual thermodynamical method of computing the multifractal spectrum of $f(t)$ is to define a partition function which scales, in the limit $a \to 0$ as

$$Z(q,a) = \sum_n \left|W_\psi[f(t)](t_n(a),a)\right|^q \approx a^{\tau(q)} \quad \ldots. (4)$$

where $t_n$ is the position of all local maxima at a fixed scale $a$ and $q$ is the moment of the measure distributed on the WTMM hierarchy used to define the power-law scaling of $Z(q,a)$. The multifractal spectrum is obtained by applying the Legendre transformations to $\tau(q)$. If there is a time series that has a monofractal structure, then we obtain a straight line in linear plot of $\tau(q)$ versus $q$. When the exponents $\tau(q)$ in Eq. (4) are in the form of straight line, the time series is a monofractal; otherwise, the time series is a multifractal [14, 15]. The $\tau$ (q) versus q curve, also called $\tau$ (q)-spectrum, shows the nonlinear dependence of the $\tau$ function on q. The vertex of the $\tau$ (q) curve becomes narrower or wider for more heterogeneous and less heterogeneous multifractal distributions, respectively. The singularity spectrum, $f(\alpha)$, approximately an upside-down parabola, peaks at $f_{\alpha,\max}$. The range $\Delta\alpha$ quantifies the fractal non-

uniformity, while $f_\alpha$ characterizes ground motions components with scaling exponent α occur. More precisely, we apply the wavelet transform modulus maxima (WTMM) method that has been proposed as a generalization of the multifractal formalism from singular measures to fractal distributions [13, 17]. By using wavelet analysis, we reveal the clear fractal characteristics of the analyzed time series and successfully describe the main features of our earthquake sequences. The study focuses on the interpretation and explanation of the various temporal fractal patterns found in earthquake time series.

## RESULTS AND DISCUSSION

In the present paper we have analyzed the Gorkha Nepal earthquake data recorded at different stations of Kathmandu valley as given in the Table 1. In this Table we have arranged the stations according to their distances from the epicenter. To get a complete multifractal spectrum, q should range from -∞ ($\alpha_{min}$) to +∞ ($\alpha_{max}$). Multifractal analysis of the earthquake data recorded at different stations of increasing distances from the earthquake epicenter has been carried out in Table 2. From the multifractal spectrum, we can draw significant conclusions about the multifractality of a time series. The singularity spectrum *f(α)* indicates the dimension of the subset of the series characterized by singularity strength α [17,18] and its width shows the range of the exponents, defined as $\Delta\alpha = \alpha_{max} - \alpha_{min}$ , where $\alpha_{max}$ and $\alpha_{min}$ are the maximum and minimum value of α [19,20]. The more or less multifractality of the series (larger or smaller $\Delta\alpha$), the more or less heterogenous the series. In the case of multifractals, the shape of the singularity spectrum typically resembles an inverted parabola, and the degree of their complexity is quantified by its width. For monofractal signals, the spectrum converges to a single point, but it is difficult to occur in common practice.

**Table 2: In this table the minimum and maximum values of the singularities have been shown for different stations according to their distance from the epicentral distance of the earthquake.**

| Earthquake recording station | Epicentral Distance (km) | Singularity Spectra(α) | | |
|---|---|---|---|---|
| | | $\alpha_{max}$(N;E;Up) | $\alpha_{min}$(N;E;Up) | $\Delta\alpha = \alpha_{max} - \alpha_{min}$ (N;E;Up) |
| KTP | 75.9 | 0.48;0.42;0.52 | -0.46;-0.56;-0.53 | 0.94;0.96;1.05 |
| TVU | 77.0 | 0.87;0.73;0.62 | -0.14;-0.18;-0.46 | 1.01;0.91;1.08 |
| PTN | 79.3 | 0.66;0.52;0.38 | -0.28;-0.28;-0.46 | 0.94;0.80;0.84 |
| THM | 83.7 | 0.52;0.56;0.34 | -0.14;-0.25;-0.53 | 0.66;0.81;0.87 |

Figure 2a, 3a, 4a and 5a show the moment generating function (τ spectrum) for all the time-series data. The curvature of the exponent function τ(q) reflects the multifractality of the time series. Note that all τ spectra are curved; indicating the earthquake ground motions are multifractal in nature. However, the τ-spectrum for the EW and NS components less curved than vertical component in all stations data. We plotted the singularity spectra $f(\alpha)$ for all components of the earthquake recording data at four different stations in Figures 2b, 3b, 4b and 5b. We note that in all the singularity spectra curves there are a stronger multifractality degree. The multifractal spectrum f(α) of the data are much broader range, confirming that the underlying dynamics of the ground motion data signal are multifractal.

Further, we analyzed three different components of the ground motion for earthquake recorded at four different stations. We found that the vertical wave motions are characterized by wider range of values of exponent $\tau_q$ and wider multifractal spectrum ($\Delta\alpha$ V =1.05, 1.08, 0.84 and 0.87) in comparison to NS and EW components except at PTN. NS and EW wave motions have same width of multifractal spectrum at KTP but differ in other stations. The maximal effects of vertical component observed in all records from these stations could be attributed to high response amplification of the structure in the vertical direction. We found large $\Delta\alpha$ observed high in vertical components and second more in EW components. It is also noted that, although the $\Delta\alpha$ parameters are much closed ($\Delta\alpha$ = 0.94 NS and $\Delta\alpha$ = 0.96 EW at KTP), the values for $\alpha_{max}$ are slightly different: $\alpha_{max}$ =0.48 (NS) and $\alpha_{max}$= 0.42 (EW). This could be due to an epicentral distance of 75.9 km along with the predominant horizontal

movement from strike-slip characteristics of ground fault. This indicates that the presence of the strong and deterministic phenomena contributes to decrease the multifractal characteristics on the time series. Moreover, the distance from the fault rupture also leads to a time lag between the arrival of peak vertical motion and peak horizontal motion. Similarly, the measured higher values of $\alpha_{max}$ were: KTP ($\alpha_{max}$= 0.52), TVU ($\alpha_{max}$= 0.87), PTN ($\alpha_{max}$= 0.66) and THM ($\alpha_{max}$=0.55). For the values of $\alpha_{min}$, the lowest values were observed: KTP ($\alpha_{mim}$ = -0.56), TVU ($\alpha_{mim}$ =-0.46), PTN ($\alpha_{mim}$ =-0.46) and THM ($\alpha_{mim}$ =-0.53). Variations in the width of singularity spectra indicate heterogeneity (Table 2), as these parameters provide information on the variability in the measured scales. Width of the f(α)-α spectrum is positively correlated with heterogeneity in the local scaling indices.

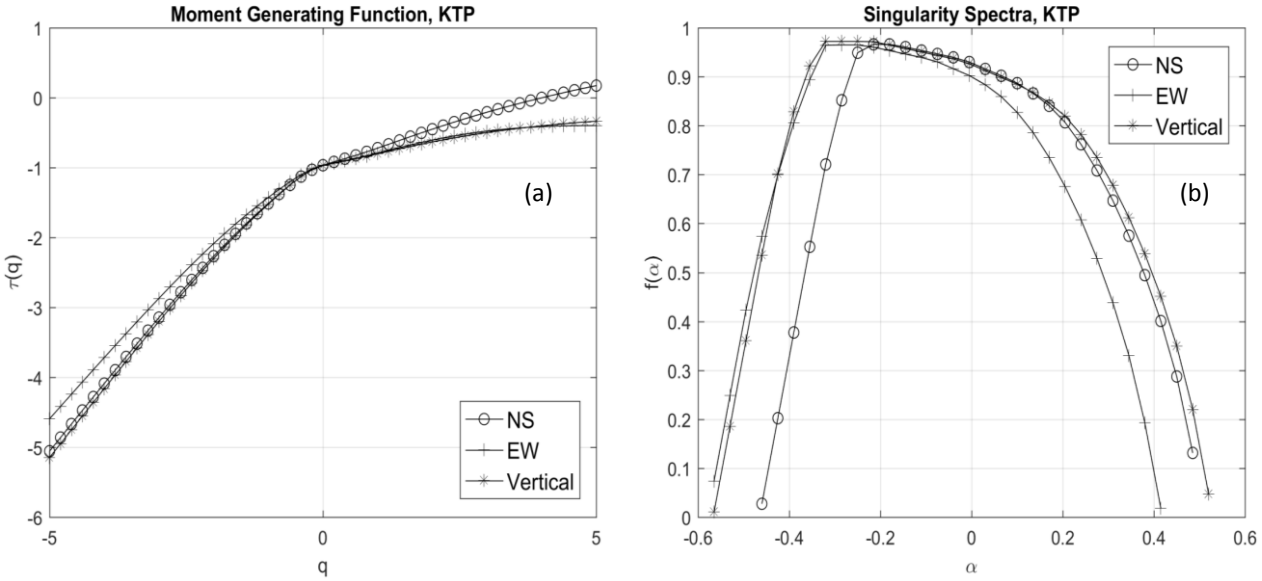


**Fig. 2:** (a) Moment generating function (Tau spectrum) for each of the three components of the earthquake accelaration data. Notice the strong similarities in the east-west and north–south components, but vertical component shows more deviation. (b) Comparisons of multifractal or singularity spectra $f(\alpha)$ representations of the earthquake data recorded at station KTP.

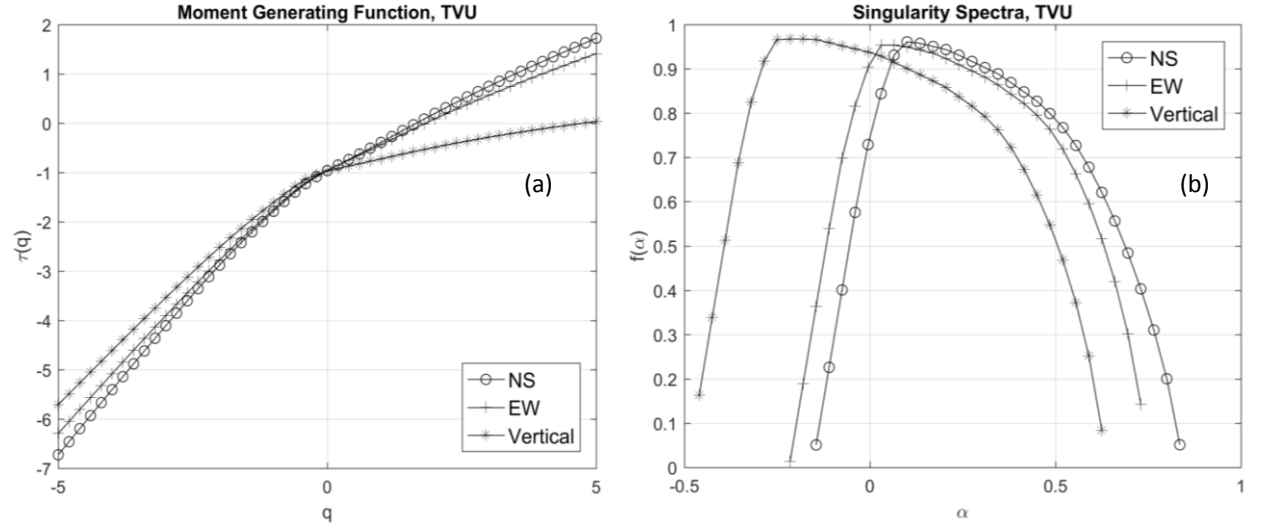


**Fig. 3:** (a) Moment generating function (Tau spectrum) for each of the three components of the earthquake acceleration data. (b) Comparisons of multifractal or singularity spectra $f(\alpha)$ representations of the earthquake data recorded at station TVU.

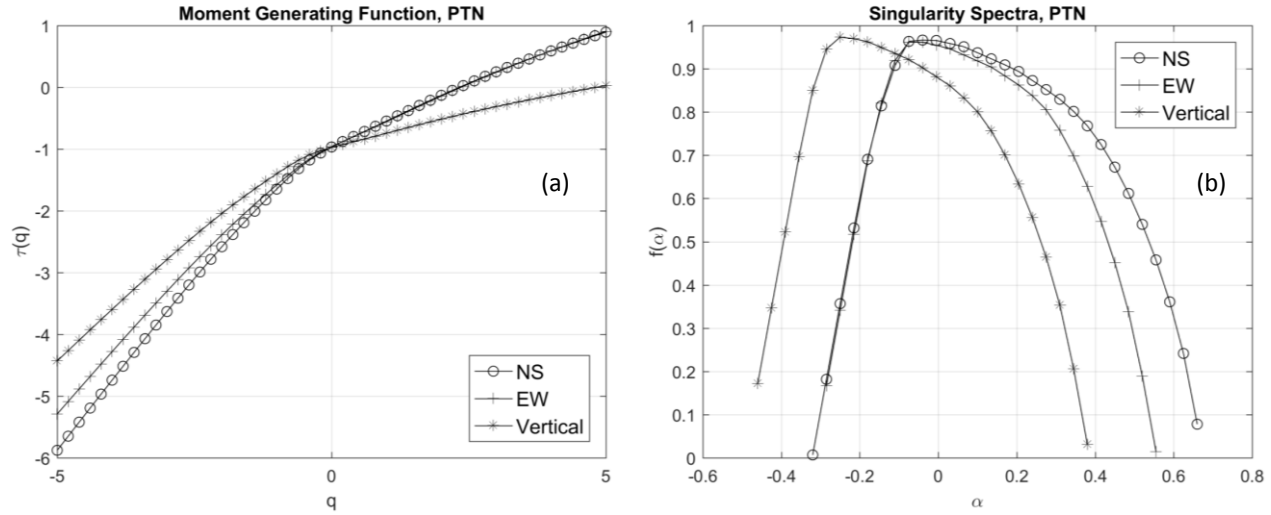


**Fig. 4:** (a) Moment generating function (Tau spectra) for each of the three components of the earthquake acceleration data. (b) Comparisons of multifractal or singularity spectra $f(\alpha)$ representations of the earthquake data recorded at station PTN.

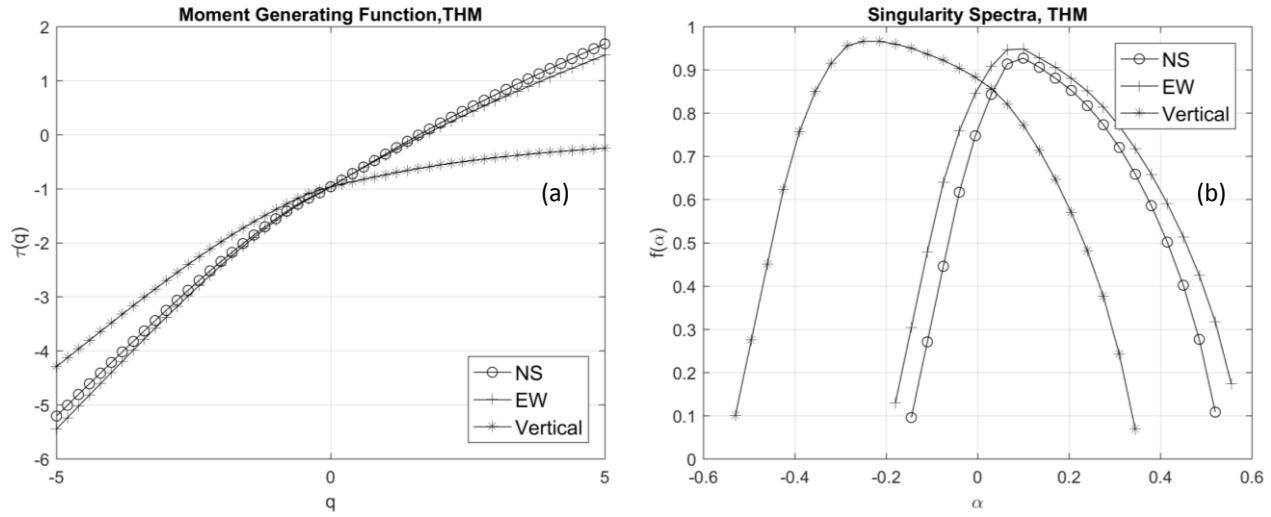


**Fig. 5:** (a) Moment generating function (Tau spectra) for each of the three components of the earthquake acceleration data. (b) Comparisons of multifractal or singularity spectra $f(\alpha)$ representations of the earthquake data recorded at station THM.

The results indicate that the singularities spectra of the spatial distribution of earthquake epicenters in the Gorkha, Nepal have multifractal structures. They show scale-invariant behavior, indicating that the spatial patterns of seismicity in these regions have multifractal structures. The variations of τq for the spatial distribution of earthquake in these regions could be the result of different underlying dynamics that may be operating in these regions. The moment generating function (τq spectrum) for all components have a gentle slope but among them vertical motions have more. This implies that vertical components are more heterogeneous than other components. The differences in the degree of heterogeneity within the multifractal distribution of earthquake epicenters in these regions are also confirmed by the relatively wider vertex of the τ(q)-spectrum. The obtained results also indicate that the multifractal seismicity patterns of these regions have asymmetrical distribution. We have clearly

seen in the f(α)- α diagrams. The relatively higher values of Δα for Kirtipur site indicate that the seismicity in this region has a rich or broad nonuniform (i.e. heterogeneous) multifractal structure denoted by a relative wide range of fractal exponents. The analysis reveals that although the spatial distributions of earthquake epicenter around 76 km distances from Kirtipur have multifractal structures, the seismicity of the Bhaktapur region has a narrow or smooth multifractal (i.e. less heterogeneous fractal) structure which is nearly 87 km far from the epicenter. This fact may reflect the differences in physics and underlying structures of the seismotectonic processes in these regions. Most earthquakes occur in weak crusts, and their occurrence has often been related to the movements of small fault segments.

## CONCLUSION

In this work, we analyzed the multifractal aspects of the Gorkha earthquake ground recording data obtained from four different stations of Nepal. The multifractal signature, characterized by a well-developed Gaussian shape on the singularity spectra, $f(\alpha)$ and obtained through use of the WTMM approach, was observed for four different sites. Some differences and similarities among sites were successfully detected. A new behavior was observed in vertical components at $f(\alpha)$ spectra. It is possible to conjecture that this behavior may be associated with some aspects of land structure, which are still poorly understood, causing the increase of the intermittence phenomena. Thus, from all the above analysis, it is concluded that existence of long-range correlations is the primary source of multifractality in these seismic signals. The singularity plots shown above represent the spectra of fractal dimension with different strength. The spectrum for vertical motion seems to be broader to that of EW and NS motions. The broader spectrum is an indicator of stronger multifractal behavior. Hence, it is inferred that there is an increase in multifractality of the signals toward the time of delivery. The multifractal features extracted from the original recorded ground motion signals are shown in Table 2. From multifractal analysis the fractal dimension of the singularity support is around one. The lower and upper bound of the singularity increase with the distances of the stations from the earthquake epicenter. It indicates that the signal becomes smoother with distances. In conclusion, the data shows a multifractal behavior, and the major event takes place in a short duration. However, despite some differences found among the sites, it is possible to characterize the common behavior found in this work through specific parameters. It should be necessary to analyze longer data sets, recorded in different tectonic settings. Thus, our next step will be finding an approach to normalize these findings for different locations with the objective of obtaining some universal parameters. This objective will allow us to model the multifractal spectral such as the p-model [21].

## ACKNOWLEDGEMENTS

The authors would like to acknowledge the Chinese Academy of Science, Beijing for financial support and State Key Laboratory of Space Weather for providing fundamental facilities. The datasets were obtained from European-Mediterranean Seismological Centre (EMSC) webpage: [http://www.emsc-sem.org/Earthquake/seismologist.php], Central Department of Geology, Tribhuvan University, University Grants Commission office, Bhaktapur, Kirtipur Municipility Office and Pulchowk Campus, Institute of Engineering, Patan. And the dataset downloaded from the web page:[http://www.strongmotioncenter.org] is for the study of ground motion. We would like to thanks for them.

## REFERENCES

[1] Subedi, S. and Poudyal Chhetri, M. B. Impacts of the 2015 Gorkha Earthquake: Lessons Learnt from Nepal, In book: Earthquakes - Impact, Community Vulnerability and Resilience, DOI: http://dx.doi.org/10.5772/intechopen.85322 (2019).

[2] Enescu, B.; Ito, K. and Struzik, Z. Wavelet-based multiscale resolution analysis of real and simulated time-series of earthquakes, Geophysical Journal International, **164**: 63–74 (2006).

[3] Lyubushin, A. A.; Kaláb, Z.; Lednická, M. and Haggag, H. M. Discrimination of earthquakes and explosions using multi-fractal singularity spectrums properties; J Seismol **17**: 975–983 (2013).

[4] Bolzan, M. J. A. and Rosa, R. R. Multifractal analysis of interplanetary magnetic field obtained during CME Events Ann. Geophys., **30**: 1107–1112 (2012).

[5] Macek, W. M. and Wawrzaszek, A. Voyager 2 observation of the multifractal spectrum in the

heliosphere and the heliosheath Nonlin. Processes Geophys, **20**: 1061–1070 (2013).

[6] Puckovs, A. and Matvejevs, A. Wavelet Transform Modulus Maxima Approach for World Stock Index Multifractal Analysis, Information Technology and Management Science December 2012 DOI: 10.2478/v10313-012-0016-5

[7] Avouac, J. P.; Meng, L.; Wei, S.; Wang, T. and Ampuero, J. P. Lower edge of locked Main Himalayan Thrust unzipped by the 2015 Gorkha earthquake; Nature; Geoscience (2015).

[8] Grandin, R.; Vallée, M.; Satriano, C.; Lacassin, R.; Klinger, Y.; Simoes, M. and Bollinger, L. Rupture process of the Mw=7.9 2015 Gorkha earthquake (Nepal): Insights into Himalayan megathrust segmentation, Geophysical Research Letters, **42**: …. (2015).

[9] Kobayashi, S.; Ota, Y.; Harada, Y.; Ebita, A.; Moriya, M.; Onoda, H.; Onogi, K.; Kamahori, H.; Kobayashi, C.; Endo, H.; Miyaoka, K.; Takahashi, K. The JRA-55 Reanalysis: General Specifications and Basic Characteristics Journal of the Meteorological Society of Japan, Vol. **93** (1): 5−48 (2015).

[10] Takai, N.; Shigefuji, M.; Rajaure, S.; Bijukchhen, S.; Ichiyanagi, M.; Dhital, M. R. and Sasatan, T. Strong ground motion in the Kathmandu Valley during the 2015 Gorkha, Nepal, earthquake Earth, Planets and Space, **68**: …….. (2016).

[11] Adhikari, B.; Dahal, S.; Karki, M.; Mishra, R. K.; Dahal, R. K.; Sasmal, S. and Klausner, V. Application of wavelet for seismic wave analysis in Kathmandu Valley after the 2015 Gorkha earthquake, Nepal Geoenvironmental Disasters (2020).

[12] Shrestha, O.; Koirala, A.; Karmacharya, S.; Pradhananga, U.; Pradhan, P.; Karmacharya, R. Engineering and environmental geological map of the Kathmandu valley. Department of Mines and Geology, Kathmandu (1998).

[13] Muzy, J. F.; Bacry, E. and Arneodo, A. Wavelets and Multifractal formalism for singular signals: Application to turbulence data, Physical Reviews. Letters, **67**: 3515–3518 (1991).

[14] Arneodo, A.; Bacry, E. and Muzy, J. F. The thermodynamics of fractals revisited with wavelets, Physica A, **213**: 232–275 (1995).

[15] Oswiecimka, P.; Kwapien, J. and Drozdz, S. Wavelet versus detrended fluctuation analysis of multifractal structures, Phys. Rev. E, **74**: 016103 (2006).

[16] Arneodo, A.; d'Aubenton-Carafa, Y.; Bacry, E.; Garves, P. V.; Muzy, J. F. and Thermes, C. Wavelet based fractal analysis of DNA sequencesPhysica D, **96** : 219-320 (1996).

[17] Turiel, A.; Pe´rez-Vicente Conrad, J.; Grazzini, J. Numerical methods for the estimation of multifractal singularity spectra on sampled data: A comparative study, *Journal of Computational Physics*, **216** : 362–390 (2006).

[18] Kantelhardt, J. W.; Zschiegner, S. A.; Koscielny-Bunde, E.; Havlin, S.; Bunde, A. and Stanley, H. E. Multifractal detrended fluctuation analysis of nonstationary time series, *Physica A*, **316**: 87–114 (2002).

[19] Padhy, S. The multi-fractal scaling behavior of seismograms based on the detrended fluctuation analysis, in Fractal solutions for understanding complex systems in Earth sciences, edited by Dimri, V. P. Springer Earth System Sciences Springer, Cham, 99–115 (2016).

[20] Imashev, S.; Mishchenko, M. and Cheshev, M. Fractal analysis of seismoacoustic signals of near-surface sedimentary rocks in Kamchatka; GEOFIZIKA, **36**: …… (2019).

[21] Halsey, T. C.; Jensen, M. H.; Kadanoff, L. P.; Procaccia, I., and Shraiman, B. I. Fractal measures and singularities – The characterization of strange sets, Physical Review A, **33**: 1141–1151 (1986).